JOURNAL OF MATERIALS SCIENCE **36** (2001) 4195–4199

Preparation, sintering and fracture behavior of $Al_2O_3/LaAl_{11}O_{18}$ ceramic composites

YI-QUAN WU, YU-FENG ZHANG, XIAO-XIAN HUANG, BAO-SHUN LI, JING-KUN GUO
State Key Lab of High Performance Ceramics and Superfine Microstructure, Shanghai Institute of Ceramics, Chinese Academy of Sciences, Shanghai 200050, People's Republic of China
E-mail: yiquanwu@netease.com

Al_2O_3/25 vol% $LaAl_{11}O_{18}$ composites were prepared by pressureless sintering at 1550°C with composite powders obtained by copercipiated method using $La(NO_3) \cdot 6H_2O$ and $Al(NO_3)_3 \cdot 9H_2O$ as starting materials. The enhanced reactive activity of Al_2O_3 and chemically homogeneous mixing of the constituents made $LaAl_{11}O_{18}$ phase to be formed at low temperature in composite powders. AlF_3 additive was used to reduce the transformation temperature of transition alumina. The $LaAl_{11}O_{18}$ grains in the composite powder obtained at 1500°C showed rodlike morphology distributed homogeneously in Al_2O_3 powder. The samples sintered at 1550°C for 4 h with CAS (CaO-Al_2O_3-SiO_2) sintering aid can obtain a high relative density. The effects of the sintering time on the grain growth of Al_2O_3 and the fracture toughness of the composites were studied and the results showed that $LaAl_{11}O_{18}$ grains reduced the growth of Al_2O_3 grains and the rodlike grains increased the fracture toughness. The improvement in fracture toughness of the composites was mainly attributed to the mechanism of crack deflection.

1. Introduction

Because of its attractive properties of high melting point, high wear resistance, excellent electrical resistively and chemical durability as well as its low cost availability of raw materials. Alumina is one of the most important materials for use in structural, electrical, optical and biomedical application [1]. However, the biggest obstacle for wider applications is its brittle failure under mechanical or thermal stress. Effects have been made to further improve its toughness and thermal shock resistance, which can be realized by *in situ* formation of second phases during sintering [2, 3]. Recently, some researchers have developed *in situ* formation platelike $LaAl_{11}O_{18}$ reinforcing Al_2O_3 composite because of its compatibility with layer aluminate compound of $LaAl_{11}O_{18}$. For example, Kanzaki [4] prepared high-strength and high-fracture-toughness $Al_2O_3/LaAl_{11}O_{18}$ composite by reaction of $LaAlO_3$ and Al_2O_3 with addition of silica sol. Chen [5] developed *in situ* formation $Al_2O_3/LaAl_{11}O_{18}$ composite by using Al_2O_3 powder and $La(NO_3)_3 \cdot 9H_2O$ as the starting materials. Kishi [6] fabricated $Al_2O_3/LaAl_{11}O_{18}$ composite by hot-pressing sintering using La_2O_3 and Al_2O_3 powders as starting materials and Messing [7] used a boehmite sol and $La(NO_3)_3 \cdot 6H_2O$ to prepare the $Al_2O_3/LaAl_{11}O_{18}$ composite by sol-gel method. These methods need either high solid synthesis temperatures or complex processing and long-time consumption, which pose some barriers to commercialization.

The objective of this study was to fabricate $Al_2O_3/LaAl_{11}O_{18}$ composites by a copercipiated method using $Al(NO_3)_3 \cdot 9H_2O$ and $La(NO_3)_3 \cdot 6H_2O$ as starting materials and this paper presented the characteristics of the synthesized powders and the sintered samples.

2. Experimental procedure

The Al_2O_3/25 vol% $LaAl_{11}O_{18}$ powders were synthesized by firstly dissolving $Al(NO_3)_3 \cdot 9H_2O$ and $La(NO_3)_3 \cdot 6H_2O$ in distilled water, respectively and then mixed to yield precipitate by adjusting the pH value of the solution to 9–10 with $NH_3 \cdot H_2O$ solution. The precipitate was aged, filtered and washed with distilled water and ethanol, respectively. After drying, the dried gel was milled with ethanol by adding a little amount of AlF_3 in high purity alumina mediums and then again dried. The composite powders can be obtained by calcining the dried gel for 1 h at different temperatures.

The composite powders obtained by calcining the dried gel for 1 h at 1200°C and 1500°C respectively, were ball-milled in ethanol for 24 h with 0.1 wt% CAS (CaO-Al_2O_3-SiO_2) sintering additive, then dried and uniaxially pressed at 500 MPa, and sintered at 1550°C for different sintering time. The average particle size of the powder after ball-milling step, analyzed using a Mastersizer 2000 Ver. analyzer, was 0.6 μm and 1.8 μm, respectively.

The powder phases were identified by X-ray diffraction (D/max-radiffractometer, Japan) with Ni filtered

Cu Kα radiation. The calcined powders and the etched sintered samples were observed using SEM (EPMA-8705QHz, Japan). TEM (JEM-400cx, JEOL, Japan) was used for the analysis of the platelike grains.

The densities of sintered samples were determined by the Archimedes method. The fracture toughness was measured by the Vickers Indentation (AKASHI). The formula used for calculating K_{IC} was expressed as $K_{IC} = A(E/H)^{1/2}(P/c^{2/3})$. A minimum of six specimens was tested to obtained a single datum. Grain size of sintered samples was measured from SEM micrographs by using the lineal intercept technique using at least 200 grains for each sample.

3. Results and discussion

3.1. The calcined powder characteristics

The XRD patterns of the gel calcined at different temperatures between 800°C and 1500°C were shown in Fig. 1. The pattern of the powder obtained at 800°C exhibited diffraction peak of γ-Al_2O_3 and amorphous background with a little amount of α-Al_2O_3 phase, and the peaks of $LaAlO_3$, $LaAl_{11}O_{18}$ and α-Al_2O_3 phase were observed by calcining dried gel at 1200°C. The

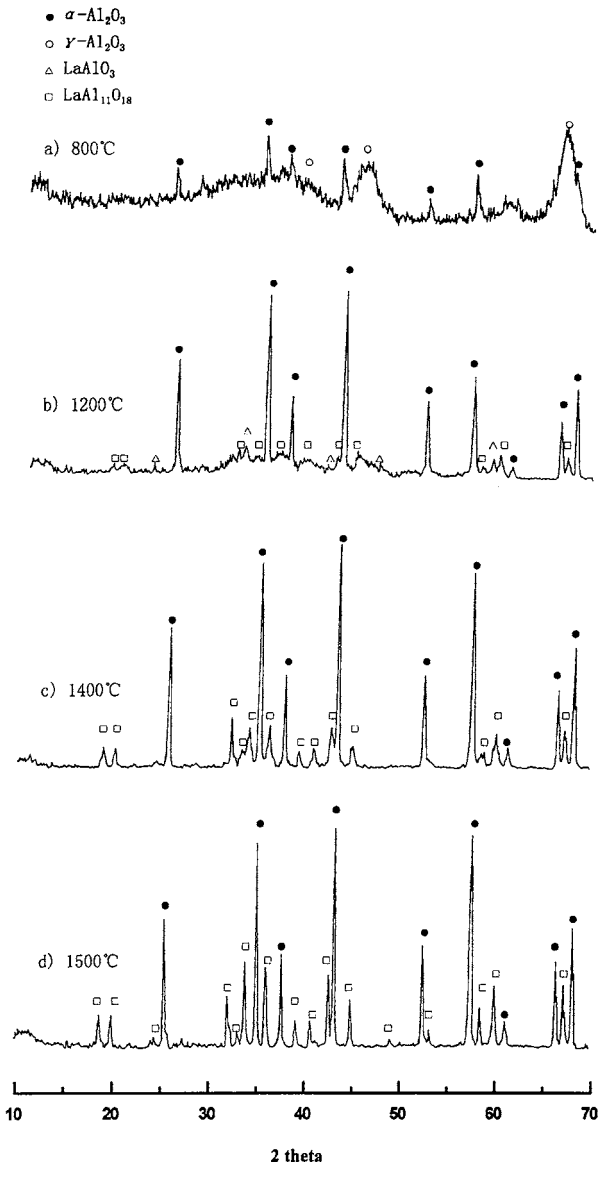

Figure 1 XRD patterns of powders calcined at different temperatures.

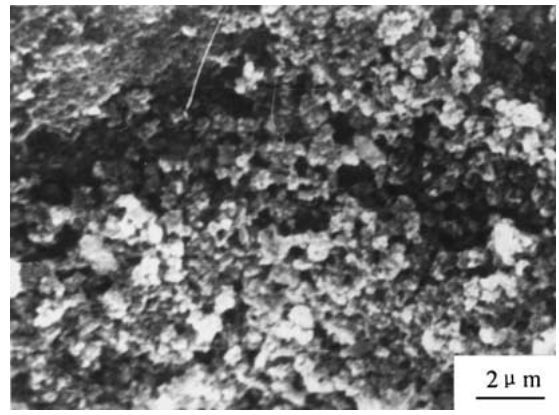

Figure 2 SEM micrograph of powder A.

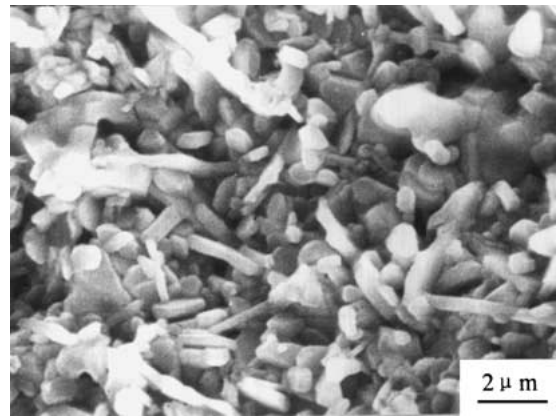

Figure 3 SEM micrograph of powder B.

SEM micrograph showed that the powder calcined at 1200°C (designated as powder A) appeared to be homogenous and consisted of small equiaxed grains with a size of 0.2 μm, as shown in Fig. 2. The patterns for the powders obtained at 1400°C and 1500°C showed well-defined peaks of $LaAl_{11}O_{18}$ and α-Al_2O_3, and the degree of crystallinity at 1500°C was much higher. It was suggested that the intermediate phase of $LaAlO_3$ formed at low temperature can be transformed into $LaAl_{11}O_{18}$ at higher temperature. La^{3+} has a stabilizing effect on the transition alumina because of its incorporation in the transition alumina [8], but the addition of AlF_3 and milling with high purity alumina mediums can reduce the transformation temperature of transition alumina [9, 10]. So transition alumina can be transformed into α-Al_2O_3 at lower temperature and enhanced the reactive activity of α-Al_2O_3 with La_2O_3 and $LaAlO_3$. The rodlike grains with average aspect ratio 3–5 distributed homogeneously in the matrix powder calcined at 1500°C (designated as powder B) can be seen from the SEM micrograph, as shown in Fig. 3, necking can be seen from the micrograph due to the higher calcining temperature. The XRD analysis and TEM indicated that the rodlike grains are $LaAl_{11}O_{18}$, as shown in Fig. 4.

3.2. The sintering and microstructural characteristics of samples

Fig. 5 shows the relative densities of samples sintered at 1550°C versus the sintering time. The theoretical density of Al_2O_3/25 vol% $LaAl_{11}O_{18}$ composite estimated by the lever rule from the true density of each

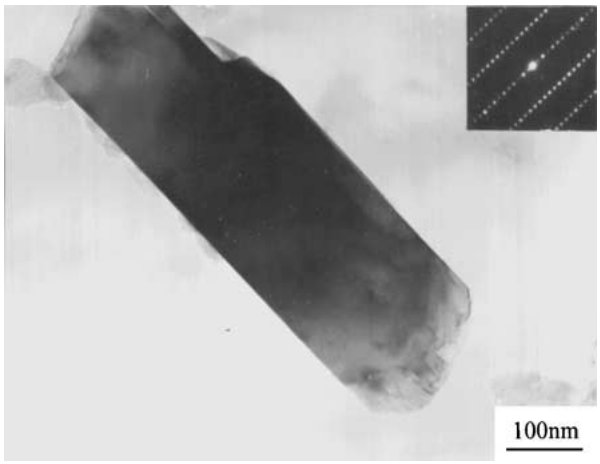

Figure 4 TEM micrograph and SAED pattern of rodlike $LaAl_{11}O_{18}$.

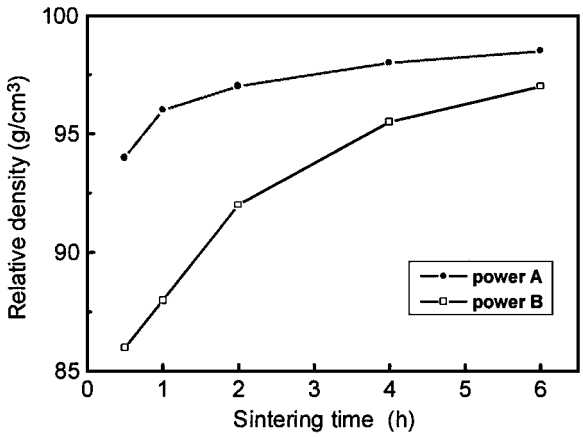

Figure 5 Relative density of the samples sintered at 1550°C.

compound (Al_2O_3: 3.98 g/cm^3, $LaAl_{11}O_{18}$: 4.17 g/cm^3) is 4.03 g/cm^3 [11]. It can be seen from Fig. 5 that the relative densities of the samples sintered with powder B at 1550°C for 4 h can reach ≥95%. It is known that an elongated second phase in matrix powder can inhibit densification and make it difficult to achieve full density [11], but in this experiment the rodlike $LaAl_{11}O_{18}$ grains distributed in Al_2O_3 composite powder prepared by copercipiated method can be sintered to a relatively high density. It was due to that the enhanced reactive activity of powders, the high shape-forming pressure and the CAS liquid-forming additive improved the densification. The composite powder A can be sintered to ≥98% because of the finer equiaxed active grains. Although small pores were present, the densities of the composites were found to be close to theoretical density, indicating that the total pore volume was very small.

The formation of $LaAl_{11}O_{18}$ in the samples sintered with powder A at 1550°C, inhibited the grain growth of Al_2O_3 and narrowed the grain size distribution, making the composite matrix more uniformly structured. The microstructure of sample sintered at 1550°C for 6 h was shown in Fig. 6. It was known that addition of CaO and SiO_2 in Al_2O_3 powder could create favorably kinetic conditions for anisotropic grain growth of Al_2O_3 during sintering [13, 14]. In this experiment the CAS additive can not make Al_2O_3 grains to be rodlike due to that the second phase $LaAl_{11}O_{18}$ inhibited the

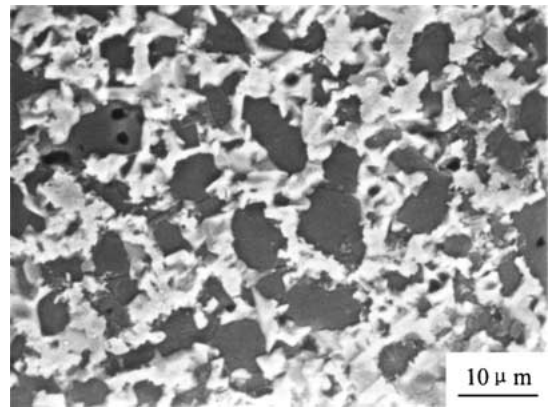

Figure 6 SEM micrograph of sample sintered with powder A at 1550°C for 6 h.

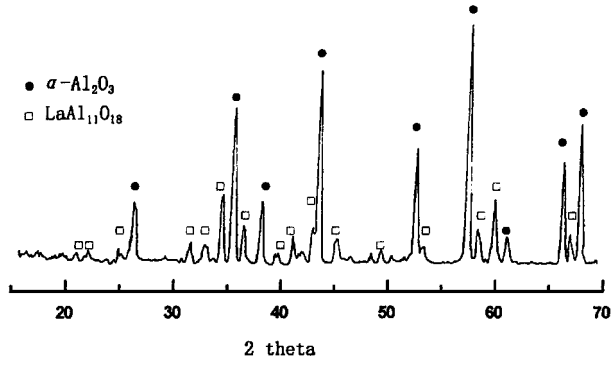

Figure 7 XRD pattern of sintered sample with powder A at 1550°C for 2 h.

grain boundary movement. But, the CAS additive was formed liquid-phase at the sintering temperature, so can promote densification of the composites. The different microstructures of samples sintered with powder A and powder B were thought to be attributed to the conditions for the synthesis and growth of $LaAl_{11}O_{18}$ grains. The formation of $LaAl_{11}O_{18}$ in powder B occurred during calcining process, $LaAl_{11}O_{18}$ grain growth had large room and was easy to became rodlike. However, the $LaAl_{11}O_{18}$ in powder A was formed during sintering green compacts, the XRD patterns shown in Fig. 7, the room was narrow and made $LaAl_{11}O_{18}$ difficult to become rodlike.

Table I shows the result of average Al_2O_3 grain size of sintered samples with power A. Fig. 8 showed the In scale relationship between the grain size and the sintering time. The above results indicated that with increasing the sintering time, Al_2O_3 grains became larger and coalescence of $LaAl_{11}O_{18}$ was formed at Al_2O_3 grain boundaries due to necking. The grain growth of Al_2O_3 is expressed by the empirical equation:

$$G^n - G_0^n = kt$$

G is grain size after time t and G_0 is the initial grain size, k is rate constants, the growth exponent, n, was

TABLE I Average Al_2O_3 grain size of the samples sintered with powder A at 1550°C

Sintering time (h)	0.5	1	2	4	6
Grain size (μm)	3.0	3.5	4.3	4.9	5.6

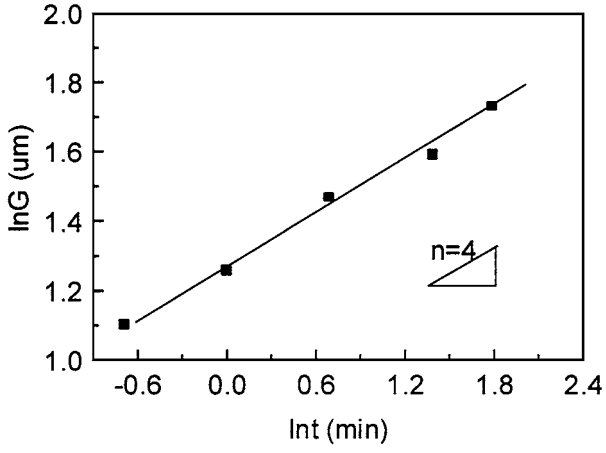

Figure 8 Ln scale dependence of Al_2O_3 average grain size of samples sintered with powder A at 1550°C on the sintering time.

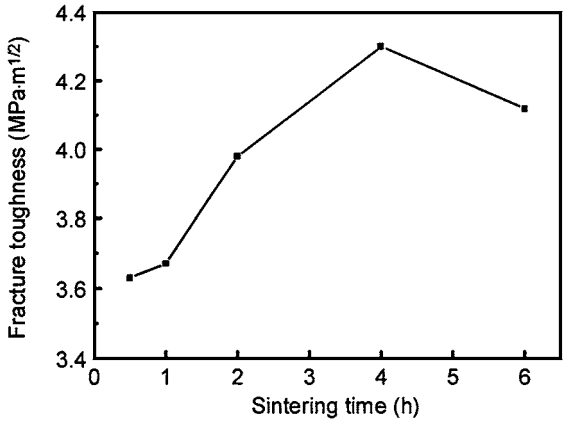

Figure 9 The fracture toughness of the samples sintered with powder B at 1550°C.

experimentally determined about $n = 4$. It indicated that the mechanism of grain growth of Al_2O_3 was boundary control through coalescence of second phase by grain boundary diffusion, because in this situation the growth exponent n is 4 [15].

3.3. The fracture behaviors of the composites

The fracture toughness of the composites prepared from powder B versus the sintering time was shown in Fig. 9. It can be noted that the fracture toughness increased with increasing the sintering time to 4 h and an optimal toughness was obtained for the composites sintered at 1550°C for 4 h. The peak toughness was attributed to the optimal interface strength between Al_2O_3 and $LaAl_{11}O_{18}$ and the grain size of Al_2O_3. It was suggested from above results that after sintering for 2 h, further prolonging the sintering time can not increase the grain size of Al_2O_3 significantly, and might make the interfaces bonding between Al_2O_3 and $LaAl_{11}O_{18}$ stronger because of interaction at the interfaces, which resulted in slighter decrease of the fracture toughness [16]. It is known that strong bonding in interfaces and finer grain microstructures show lower fracture toughness [17]. The SEM image of the crack traces introduced by Vickers Indentation on the surface of the composite sintered with powder B at 1550°C for 4 h was illustrated

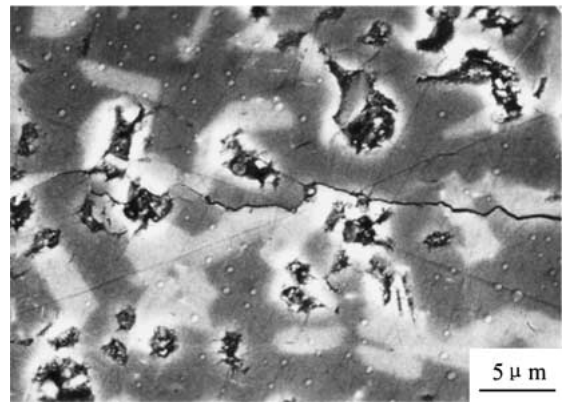

Figure 10 SEM micrograph of the crack propagation of the sample sintered with powder B.

in Fig. 10. The distribution of $LaAl_{11}O_{18}$ was quite uniform and can be easily distinguished because they contain lanthanum, resulting in bright image. The results revealed that the crack propagated through $LaAl_{11}O_{18}$ phase, deflected around coalesced $LaAl_{11}O_{18}$ and along phase interface because of weak bonding to the matrix.

4. Conclusions

1. Rodlike $LaAl_{11}O_{18}$ grains distributed homogeneously in Al_2O_3 powder can be synthesized by calcining the dried gel at 1500°C for 1 h and finer equiaxed $LaAlO_3$, $LaAl_{11}O_{18}$ and α-Al_2O_3 grains were formed at 1200°C. The gel was obtained by a coprecipitated method using $Al(NO_3)_3 \cdot 9H_2O$ and $La(NO_3)_3 \cdot 6H_2O$ as the starting materials.

2. The composite powders obtained at 1200°C (powder A) and 1500°C (powder B) can be sintered to a high density at 1550°C for 4 h with the CAS additive. The sinterability of powder A was better than powder B because of the finer equiaxed grains. The SEM results showed that powder A and B had different microstructures, because of different characters of the composite powders.

3. The *in situ* reinforced $Al_2O_3/LaAl_{11}O_{18}$ composites were fabricated using the powder B and the composites sintered at 1550°C for 4 h exhibited a peak toughness of 4.3 ± 0.4 MPa $\cdot$ m$^{1/2}$. This was mainly due to that the rodlike $LaAl_{11}O_{18}$ grains made the crack to deflect.

4. *In situ* synthesis reinforcements in matrix is an effective and promising approach to fabricate the whisker or platelets reinforced composites and can overcome the shortcomings of the conventional processes.

References

1. H. K. BOWEN, *Mater. Res. Soc. Symp. Proc.* **24** (1984) 1.
2. P. F. BECHER, *J. Am. Ceram. Soc.* **74** (1991) 255.
3. P. PENA, H. WOHLFROMM, R. TORRECILLAS and J. S. MOYA, *Ceram. Int.* **16** (1990) 375.
4. M. YASUOKA, K. M. HIRAO, E. BRITO and S. KANZAKI, *J. Am. Ceram. Soc.* **78** (1995) 1853.
5. P.-L. CHEN and I.-W. CHEN, *ibid.* **75** (1992) 2610.
6. B. K. JANG and T. KISHI, *J. Ceram. Soc. Jpn.* **106** (1998) 739.
7. C. B. SOLANO, L. ESQUIVIAS and G. L. MESSING, *J. Am. Ceram. Soc.* **82** (1999) 1318.

8. S. BRAUN, L. G. APPEL, L. B. ZINNER and M. SCHMAL, *Brit. Ceram. Trans.* **98** (1999) 77.
9. Y. YOSHIZAWA and F. SAITO, *J. Ceram. Soc. Jpn.* **104** (1996) 668.
10. K. DAIMON and E. KATO, *J. Cryst. Growth* **75** (1986) 348.
11. N. LYI, Z. INOUE, S. TAKEKAWA and S. KIMURA, *J. Solid State Chem.* **54** (1984) 70.
12. S. SUNDARESAN and I. A. AKSAY, *J. Am. Ceram. Soc.* **73** (1990) 54.
13. H. SONG and R. L. COBLE, *ibid.* **73** (1990) 2077.
14. W. A. KAYSSER, M. SPRISSIER, C. A. HANDWERKER and J. E. BLENDELL, *ibid.* **70** (1987) 339.
15. R. J. BROOK, in "Controlled Grain Growth," edited by F. Y. Wang (Treatise on Materials Science and Technology, New York, 1976) p. 331.
16. K. KAGEYAMA, M. ENOKI and T. KISHI, *J. Ceram. Soc. Jpn.* **103** (1995) 205.
17. A. G. EVANS, *J. Am. Ceram. Soc.* **73** (1990) 187.

Received 21 June 2000
and accepted 21 January 2001